Geophys. J. Int. (1997) **129**, 176–182

On the construction of geomagnetic timescales from non-prejudicial treatment of magnetic anomaly data from multiple ridges

Stephen P. Huestis[1] and Gary D. Acton[2]

[1] *Department of Earth and Planetary Sciences, University of New Mexico, Albuquerque,* NM 87131, *USA*
[2] *ODP/Texas A&M University,* 1000 *Discovery Drive, College Station,* TX 77845, *USA*

Accepted 1996 December 3. Received 1996 October 18; in original form 1996 May 23

SUMMARY

When marine magnetic-anomaly data are used to construct geomagnetic polarity timescales, the usual assumption of a smooth spreading-rate function at one seafloor spreading ridge forces much more erratic rate functions at other ridges. To eliminate this problem, we propose a formalism for the timescale problem that penalizes non-smooth spreading behaviour equally for all ridges. Specifically, we establish a non-linear Lagrange multiplier optimization problem for finding the timescale that (1) agrees with known chron ages and with anomaly-interval distance data from multiple ridges and (2) allows the rate functions for each ridge to be as nearly constant as possible, according to a cumulative penalty function. The method is applied to a synthetic data set reconstructed from the timescale and rate functions for seven ridges, derived by Cande & Kent (1992) under the assumption of smooth spreading in the South Atlantic. We find that only modest changes in the timescale (less than 5 per cent for each reversal) are needed if no one ridge is singled out for the preferential assumption of smoothness. Future implementation of this non-prejudicial treatment of spreading-rate data from multiple ridges to large anomaly-distance data sets should lead to the next incremental improvement to the pre-Quaternary geomagnetic polarity timescale, as well as allow a more accurate assessment of global and local changes in seafloor spreading rates over time.

Key words: geomagnetic reversals, inverse problem, magnetic anomalies, seafloor spreading.

INTRODUCTION

The South Atlantic has played a special role in the development of the geomagnetic polarity timescale since the pioneering work of Heirtzler *et al.* (1968). They used marine magnetic anomalies to extend the continentally derived timescale back by a factor of over 20, under the assumption of a constant spreading rate for the South Atlantic. With the addition of new calibration ages and more magnetic anomaly data, it has become clear as the timescale has evolved that the data cannot support constant spreading in the South Atlantic. Yet, in subsequent timescale revisions, this assumption has been relaxed reluctantly and minimally, to a South Atlantic with a piecewise-constant rate function involving few discontinuities, or to otherwise smooth behaviour. In their recent timescale revision, Cande & Kent (1992) summarize this evolution and present a new timescale still tied to a preferentially treated South Atlantic, whose rate function is forced to be a very smooth function of time, regardless of what this implies for rates at other ridges.

Although this represents a logical step away from the overly severe demand of constant spreading, the resulting timescale continues to force erratic variation of rate functions derived from magnetic anomaly profiles over all other ridges. In Fig. 42 of Cande & Kent (1992), the South Atlantic stands out as a ridge whose rate function is anomalously smooth. But, if the physical processes of seafloor spreading are common to all ridges, there is no convincing reason to expect one ridge to behave so differently from all others. Indeed, Wilson (1993) recently observed that spreading-rate functions for several major spreading centres have been similarly smooth over the past 5 Ma.

Here we propose a formalism for using anomaly data to estimate both the timescale and rate functions for several ridges, under a principle of 'least favouritism', wherein no one ridge is singled out as the smoothly varying ridge to which the timescale is tied. Instead, we penalize rate-function variation equally for all ridges involved; a timescale is derived with all ridges simultaneously spreading as smoothly as possible. We treat only one measure of smoothness, but note that this is

but one example of a more general approach, involving considerable flexibility in how smoothness is defined. Elsewhere, we have investigated other smoothness criteria, which were incorporated into an alternate genetic algorithm optimization method (Acton & Huestis 1994).

THEORY

Suppose that magnetic anomaly reversal locations are available from m ridges, spanning a total of K successive polarity intervals. For each ridge, distance data comprise widths of some subset of, but not necessarily all of, these intervals, measured in the direction of spreading on one side of the ridge. The ith ridge spreads with some unknown half-rate function $v_i(t)$, over the time, t, spanned by these intervals. For this ridge, denote by K_i the subset of K for which interval widths are measured. These widths are then

$$d_{il} = \int_{I_l} v_i(t)\, dt, \qquad i = 1, \ldots, m;\ l \in K_i, \tag{1}$$

with I_l the unknown duration of the lth interval. We seek to recover both $\{v_i(t); i = 1, \ldots, m\}$ and $\{I_l; l = 1, \ldots, K\}$ (or, equivalently, reversal times) from these data constraints, but this non-linear inverse problem is inescapably non-unique. For example, we know from the work of Heirtzler *et al.* (1968) that we can simply specify one ridge's rate as constant, infer the consequent polarity interval durations, then construct piecewise-constant rate functions for the remaining ridges from this timescale. Here, we instead construct one of a family of extremal solutions that do not single out any one ridge for special treatment.

To this end, express each rate function as an unknown constant, plus a non-constant residual function:

$$v_i(t) = a_i + r_i(t), \qquad i = 1, \ldots, m. \tag{2}$$

We wish to find that timescale for which all rate functions are simultaneously as simple as possible, in the sense of departing minimally from constant spreading over the intervals for which constraining distance data exist. For convenience, scale time so that the K intervals span $[0, 1]$; calibration points will eventually be required to convert results to actual time. We choose to minimize the functional

$$U = \sum_{i=1}^{m} \sum_{l \in K_i} \left\{ \int_{I_l} [r_i(t)]^2\, dt \right\} \equiv \sum_{i=1}^{m} \left\{ \int_{T_i} [r_i(t)]^2\, dt \right\}, \tag{3}$$

where T_i is the subset of $[0, 1]$ corresponding to K_i. The unknown $\{a_i, r_i(t), I_l\}$ that optimize U must satisfy

$$a_i I_l + \int_{I_l} r_i(t)\, dt = d_{il}, \qquad i = 1, \ldots, m;\ l \in K_i, \tag{4}$$

and

$$\sum_{l=1}^{K} I_l = 1, \tag{5}$$

a Lagrange multiplier problem giving non-linear simultaneous equations for these unknowns. This choice of extremal solution is a non-linear example of semi-norm minimization, propounded by Parker (1994). Solution of the Lagrange multiplier equations can be simplified if we can deduce the mathematical form assumed by the residual function at the extremum of U. This is achieved by temporarily assuming the I_l are known. If so, we could optimize

$$U' = \sum_{i=1}^{m} \left\{ \int_{T_i} [r_i(t)]^2\, dt \right\} + \sum_{i=1}^{m} \sum_{l \in K_i} \lambda_{il} \left\{ a_i I_l + \int_{T_i} [r_i(t) G_l(t)]\, dt \right\} \tag{6}$$

with respect to variations of a_i and $r_i(t)$. The λ_{il} are Lagrange multipliers, and $G_l(t)$ is a boxcar function equal to 1 over I_l, and zero elsewhere. Setting equal to zero the variations of U' with respect to $r_i(t)$, we find

$$r_i(t) = -\frac{1}{2} \sum_{l \in K_i} \lambda_{il} G_l(t), \qquad i = 1, \ldots, m. \tag{7}$$

Each residual is a step function, with discontinuities only at reversal times.

Returning to the actual problem, suppose the unknowns $\{a_i, r_i(t), I_l\}$, optimizing U subject to the constraints, have somehow been found. Any combination of perturbations to a nearby solution gives a larger U, specifically including perturbations holding the I_l fixed. For such perturbations the above argument is relevant, so that for the extremal solutions, the residual functions are still step functions with discontinuities only at reversal times; the difference is now that these times, or equivalently the I_l, are initially unknown.

Each $r_i(t)$ can thus be expressed as a set of numbers $\{r_{il}; i = 1, \ldots, m;\ l \in K_i\}$, representing their constant values along each interval. The Lagrange multiplier problem then arises from the optimization of

$$U = \sum_{i=1}^{m} \sum_{l \in K_i} \{r_{il}^2 I_l + \lambda_{il} I_l (a_i + r_{il})\} + \mu \sum_{i=1}^{K} I_l \tag{8}$$

with respect to variations in $\{a_i, r_{il}, I_l\}$. With some algebraic manipulation and elimination we reach a set of simultaneous non-linear equations:

$$\sum_{l \in K_i} [d_{il} - a_i I_l] = 0, \qquad i = 1, \ldots, m, \tag{9}$$

$$\sum_{i_l} [d_{il}^2 - a_i^2 I_l^2] - \mu I_l^2 = 0, \qquad l = 1, \ldots, K, \tag{10}$$

$$\sum_{l=1}^{K} I_l = 1, \tag{11}$$

where the sum over i_l implies summation only over ridges for which distance data for the lth interval are available. Previously eliminated to reach (9)–(11), we then have

$$r_{il} = d_{il}/I_l - a_i, \qquad i = 1, \ldots, m;\ l \in K_i. \tag{12}$$

Note, this requires that no I_l be zero, an assumption already made to eliminate the λ_{il} on the way to (9)–(11).

Some numerical method must be chosen to solve (9)–(11); we have elected to use Broyden's multidimensional secant method (Press *et al.* 1992). Of course, systems of non-linear equations might have multiple solutions; the one to which a numerical method converges might depend on the chosen starting point. We have not explored the possibility of multiple solutions, but are content with the fact that we find solutions that represent small changes to previous time-scales, and do not exhibit non-physical components such as negative rates or negative I_l values. Indeed, the original problem should have imposed additional inequalities such as $I_l \geq 0$, but we merely verify this in hindsight.

Table 1. Normal polarity intervals, Ma.

Cande and Kent (1995)	This Study	Polarity Chron
0.000 - 0.780	0.000 - 0.780	C1n
0.990 - 1.070	0.979 - 1.042	C1r.1n
1.770 - 1.950	1.789 - 2.010	C2n
2.140 - 2.150	2.219 - 2.250	C2r.1n
2.581 - 3.040	2.613 - 3.083	C2An.1n
3.110 - 3.220	3.158 - 3.256	C2An.2n
3.330 - 3.580	3.363 - 3.599	C2An.3n
4.180 - 4.290	4.096 - 4.208	C3n.1n
4.480 - 4.620	4.354 - 4.542	C3n.2n
4.800 - 4.890	4.743 - 4.835	C3n.3n
4.980 - 5.230	4.968 - 5.230	C3n.4n
5.894 - 6.137	5.912 - 6.157	C3An.1n
6.269 - 6.567	6.291 - 6.595	C3An.2n
6.935 - 7.091	6.971 - 7.131	C3Bn
7.135 - 7.170	7.177 - 7.212	C3Br.1n
7.341 - 7.375	7.388 - 7.423	C3Br.2n
7.432 - 7.562	7.482 - 7.615	C4n.1n
7.650 - 8.072	7.705 - 8.144	C4n.2n
8.225 - 8.257	8.302 - 8.335	C4r.1n
8.699 - 9.025	8.796 - 9.140	C4An
9.230 - 9.308	9.359 - 9.444	C4Ar.1n
9.580 - 9.642	9.739 - 9.806	C4Ar.2n
9.740 - 9.880	9.913 - 10.064	C5n.1n
9.920 - 10.949	10.107 - 11.168	C5n.2n
11.052 - 11.099	11.274 - 11.323	C5r.1n
11.476 - 11.531	11.714 - 11.770	C5r.2n
11.935 - 12.078	12.189 - 12.337	C5An.1n
12.184 - 12.401	12.443 - 12.666	C5An.2n
12.678 - 12.708	12.918 - 12.945	C5Ar.1n
12.775 - 12.819	13.006 - 13.047	C5Ar.2n
12.991 - 13.139	13.203 - 13.338	C5AAn
13.302 - 13.510	13.488 - 13.676	C5ABn
13.703 - 14.076	13.851 - 14.175	C5ACn
14.178 - 14.612	14.264 - 14.638	C5ADn
14.800 - 14.888	14.800 - 14.891	C5Bn.1n
15.034 - 15.155	15.039 - 15.164	C5Bn.2n
16.014 - 16.293	16.039 - 16.341	C5Cn.1n
16.327 - 16.488	16.378 - 16.551	C5Cn.2n
16.556 - 16.726	16.624 - 16.807	C5Cn.3n
17.277 - 17.615	17.399 - 17.748	C5Dn
18.281 - 18.781	18.433 - 18.906	C5En
19.048 - 20.131	19.157 - 20.211	C6n
20.518 - 20.725	20.586 - 20.771	C6An.1n
20.996 - 21.320	21.013 - 21.302	C6An.2n
21.768 - 21.859	21.701 - 21.782	C6AAn
22.151 - 22.248	22.041 - 22.128	C6AAr.1n
22.459 - 22.493	22.315 - 22.347	C6AAr.2n
22.588 - 22.750	22.436 - 22.588	C6Bn.1n
22.804 - 23.069	22.639 - 22.886	C6Bn.2n
23.353 - 23.535	23.151 - 23.415	C6Cn.1n
23.677 - 23.800	23.621 - 23.800	C6Cn.2n
23.999 - 24.118	24.015 - 24.144	C6Cn.3n
24.730 - 24.781	24.808 - 24.863	C7n.1n
24.835 - 25.183	24.922 - 25.282	C7n.2n
25.496 - 25.648	25.606 - 25.764	C7An
25.823 - 25.951	25.946 - 26.061	C8n.1n
25.992 - 26.554	26.098 - 26.618	C8n.2n
27.027 - 27.972	27.056 - 28.066	C9n
28.283 - 28.512	28.365 - 28.642	C10n.1n
28.578 - 28.745	28.718 - 28.909	C10n.2n
29.401 - 29.662	29.663 - 29.930	C11n.1n
29.765 - 30.098	30.037 - 30.380	C11n.2n
30.479 - 30.939	30.771 - 31.179	C12n
33.058 -	33.058 -	C13n

To convert the scaled interval durations (or reversal times) to actual time units, two calibration points are required. For our application below, scaled time $t = 0$ will always correspond to 0 Ma, i.e. ridge axes; then, one other reversal calibration age will convert I_l to Ma, and $v_i(t)$ to Km Ma^{-1}. Often, however, additional calibration times are credible and should be used to further constrain the extremal solution. These can be expressed as additional relations among the I_l, readily

incorporated into the Lagrange multiplier formalism. Additional calibration ages do not change the step-function nature of the residuals, just the times of those steps.

An important reminder is warranted here that the rate functions arising from the optimization will contain artefacts that are consequences of the extremal nature of the solution, without necessarily having significance beyond that. Thus, while it is a true property that the extremal solution rates have steps only at reversal times, this is clearly not required of the actual rates: they might have discontinuities at other times, or be smoothly varying. Likewise, the coupling of multiple ridges in the optimization will inevitably lead to correlations that characterize extremal solution rate functions, but not necessarily the actual rates. For example, an actual abrupt rate change on a single ridge would be distributed among all ridges as more subdued jumps, as the optimization tries to force all rates to be as close as possible to constants. We must avoid the temptation to overinterpret the details of the extremal solution. We have simply placed one bound on the solution set: the multiple ridges cannot simultaneously spread at rates closer to constants, in the specific sense defined here.

Indeed, this measure of solution simplicity is but one of many choices available to us. For example, different ridges could be assigned different positive weights $\{w_i; i = 1, \ldots, m\}$, with (3) replaced by

$$U = \sum_{i=1}^{m} \sum_{l \in K_i} w_i \int_{I_l} [r_i(t)]^2 \, dt, \tag{13}$$

or we could penalize rate-function behaviour deviating from linear, quadratic, or piecewise-constant variation. The last of these might be of particular interest if we expect ridges to have a tendency to spread at nearly constant rates for long intervals, separated by sudden rate changes. Penalizing departure from such piecewise-constant behaviour could be incorporated into this formalism, if the discontinuity times are specified at the outset. Then, the constants a_i of (2) would be replaced by separate unknown constants for each interval on each ridge. In any case, this type of extremal solution construction obviates the need to tie results to any special treatment of one particular ridge, and each different extremal solution places a valid (but not necessarily tight) bound on the solution set.

Finally, a complete formalism must admit uncertainty both in distance data and calibration ages. In the most straightforward extension, we might impose non-probabilistic hard bounds on these uncertainties (e.g. Backus 1988), whereby, for example, each data constraint (4) could be replaced by a pair of inequalities representing specification of distance uncertainty as

$$d'_{il} \le d_{il} \le d''_{il}, \qquad i = 1, \ldots, m; \, l \in K_i. \tag{14}$$

The Lagrange multiplier problem is then modified, but presents no new conceptual ideas. Alternatively, and probably preferably, incorporation of a true statistical treatment of data uncertainty might be attempted within this formalism. The purpose of this preliminary note, however, is only to suggest a general framework for the timescale problem, based upon whatever non-prejudicial extremal solution is deemed appropriate. In the example to follow, we illustrate the changes to the timescale that might result from this new approach, using a synthetic data set. A proper statistical treatment of uncertainty must wait for more complete studies, employing actual data sets.

EXAMPLE

These notions are illustrated with a synthetic data set of distances derived from the rate function for seven ridge-crest segments, given in Fig. 42 of Cande & Kent (1992): East Pacific Rise, Chile Rise, south and north Pacific, Southeast Indian Ridge, south and central Atlantic. Specifically, from these rate functions, and their timescale, we constructed corresponding distance data for polarity intervals back to 33 Ma, for a total of $K = 126$ intervals. Only two ridge segments, the south and central Atlantic, have synthetic data for each interval; the rest miss some data for either older or younger intervals, but have no intermediate data gaps in any case. It should be noted that for the ith ridge this process of synthetic data construction might fill in some gaps in the original data set of

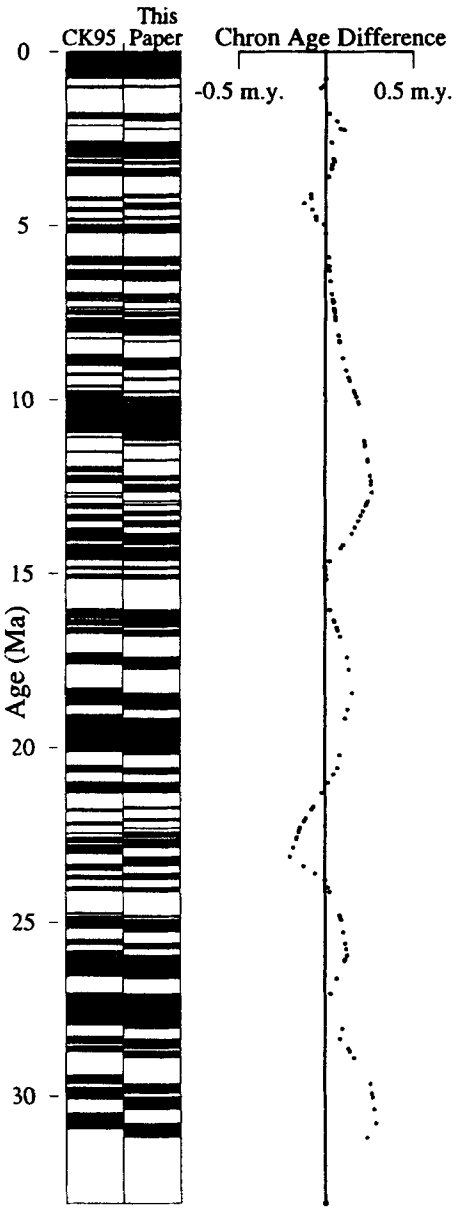

Figure 1. Comparison of the timescale of Cande & Kent (1995) with the revision of this paper. Age differences for each reversal (revised age minus age from Cande and Kent) are plotted as points on the right of the figure.

Cande & Kent by assigning distance values to all polarity intervals falling between the lower and upper limits of T_i (eq. 3). Some of the distances are thus artefacts that are not actually resolved in the original profiles. They are, however, the best estimates that can be obtained from interpolation of the distances measured by Cande & Kent.

Five calibration points were imposed, taken from the revised timescale of Cande & Kent (1995): 0.78 Ma, 5.23 Ma, 14.8 Ma, 23.8 Ma and 33.058 Ma. Table 1 lists the timescale of Cande & Kent (1995) with their chron nomenclature and the revision constructed here. Changes are modest, the largest being an increase in age at chron C12n by 0.292 Ma, from 30.479 to 30.771 Ma. The largest relative change is a 4.65 per cent increase from 2.15 to 2.25 Ma at chron C2r.1n. In Fig. 1, the two timescales are displayed pictorially, along with the age difference for each reversal.

Figs 2 to 8 show plots, for each ridge segment, of the original Cande & Kent rate function (light lines) overlain by our revised extremal-solution rate functions (heavy lines). While there are no major changes in form, the effect of applying impartial smoothness demands on all ridges is clearly seen. The new rate function for the South Atlantic is rougher than the Cande & Kent rate function, while the variability in the North Pacific, for example, has been somewhat subdued. While first-order spreading-rate variations are still present (for example, around 25 Ma in the North Pacific, or around 5 Ma on the East Pacific Rise), the smaller-scale jaggedness of rate functions is now similar in magnitude for all ridges.

Table 2 lists for each ridge the value of the residual size, $\int_{T_i} [r_i(t)]^2\, dt$ (see eq. 3) for the rate functions of Cande & Kent (1992) and the extremal solution rates of this study. Totals are also given, corresponding to the minimized functional. The total must necessarily be smaller for the extremal solution, but we also note that, as might be expected, the individual value for the south Atlantic has increased, while values for most other ridges have decreased. The central Atlantic is an exception, whose residual is larger for the extremal solution. These results are consistent with visual inspections of changes in roughness from Figs 2–8.

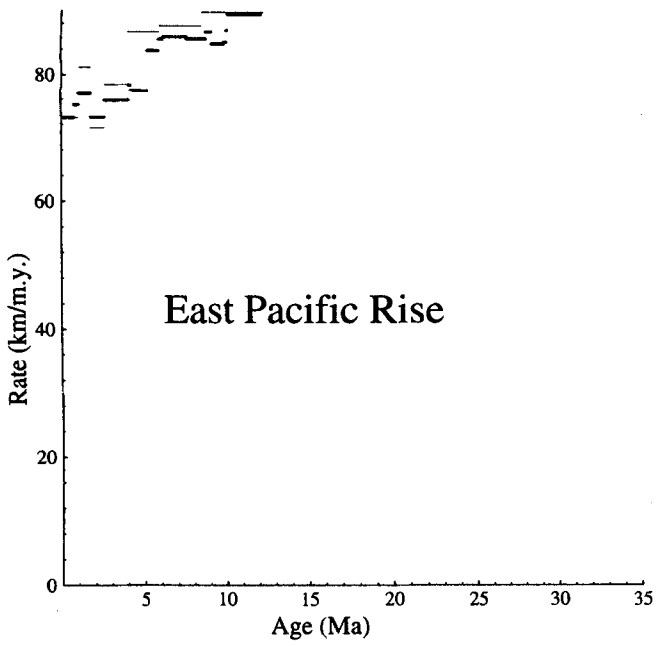

Figure 2. Spreading half-rate functions for the East Pacific rise. The rate function of Cande & Kent (1992) is shown with light lines; bold lines show the extremal-solution rate function of this paper.

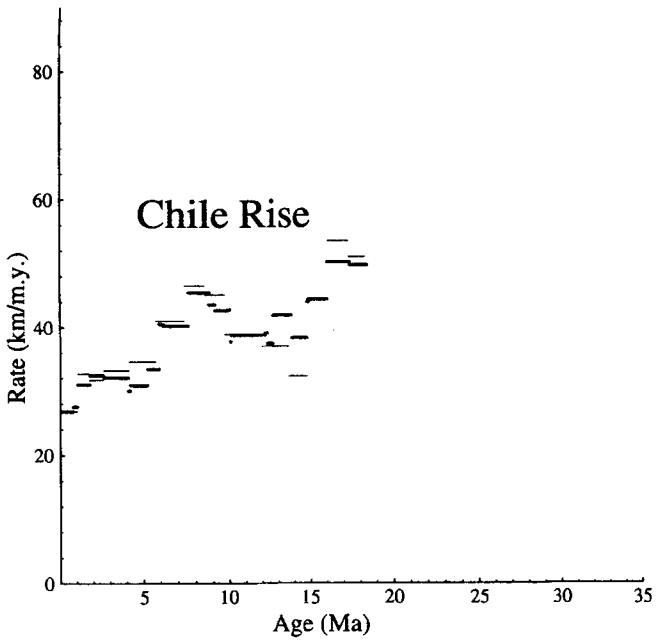

Figure 3. Same as Fig. 2 for the Chile Rise.

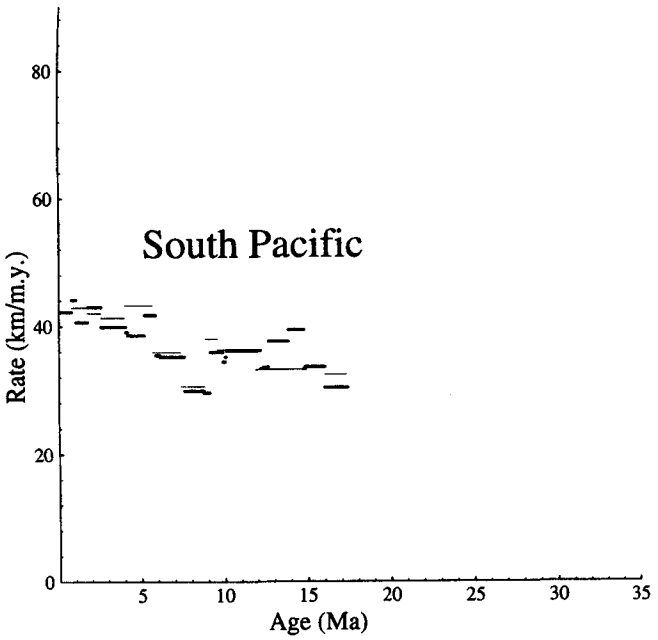

Figure 4. Same as Fig. 2 for the South Pacific.

DISCUSSION

The notions presented here allow abandonment of a lingering crutch for geomagnetic timescale development: the need to impose an artificial smoothness constraint on the spreading rate function of a single ridge. From a collection of magnetic anomaly distance intervals from more than one ridge, we have proposed finding a timescale and rate functions such that some

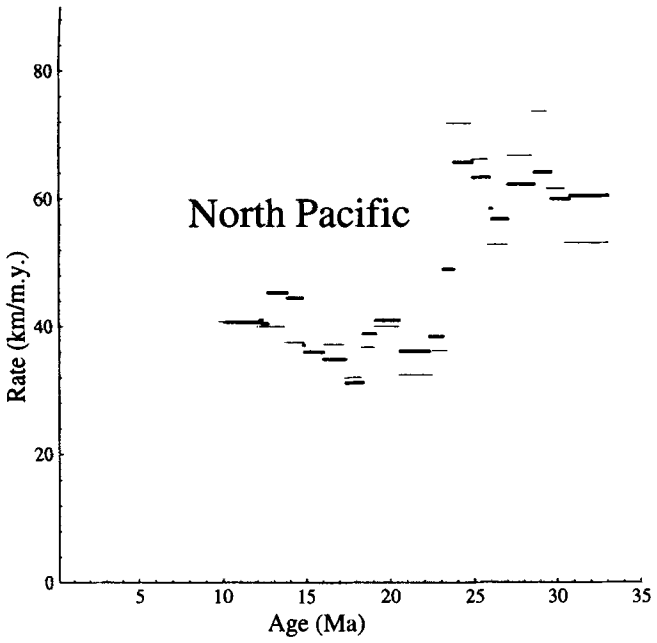

Figure 5. Same as Fig. 2 for the North Pacific.

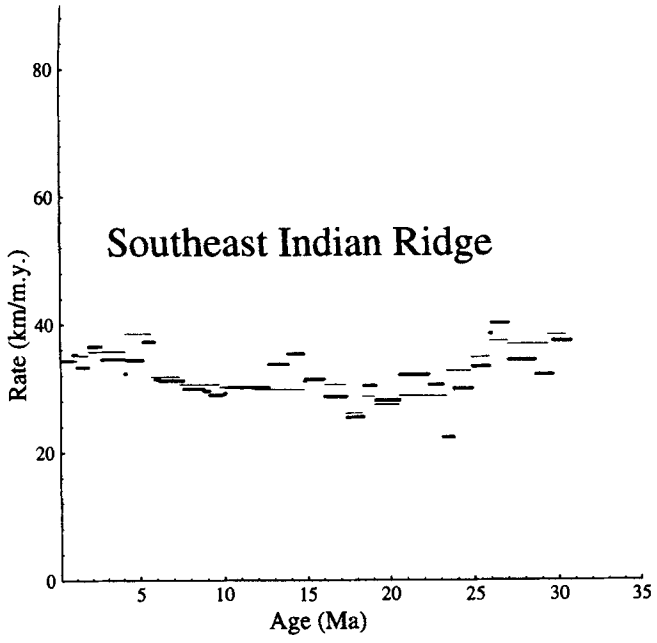

Figure 6. Same as Fig. 2 for the Southeast Indian Ridge.

cumulative measure of rate function roughness is minimized, with non-smooth behaviour of each ridge contributing to this penalty function. For the example presented here, using synthetic data reconstructed from the results of Cande & Kent (1992), we sought to force all ridges to spread with rate functions departing as little as possible from constants. The results are gratifying in that they represent only modest changes to the Cande & Kent conclusions, rather than a drastic overthrow of prior work. This argues for a more complete development and application of these ideas as a next step in the series of gradual refinements that have characterized the timescale problem for the three decades following the landmark paper of Heirtzler *et al.* (1968).

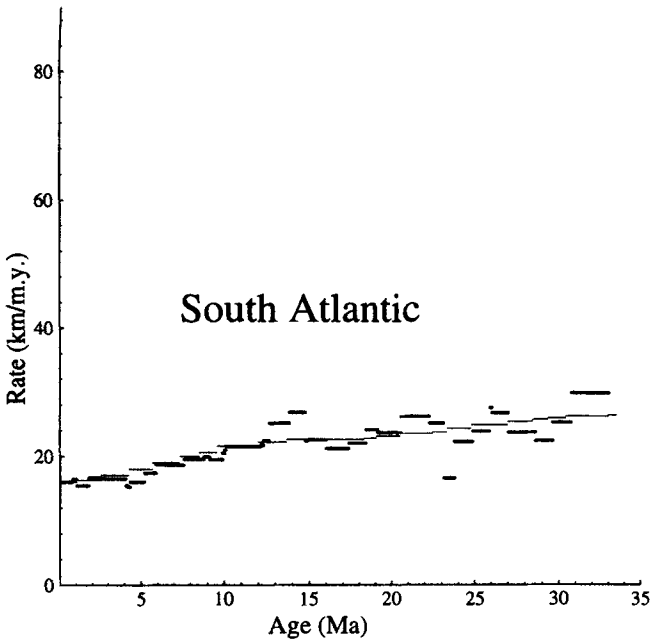

Figure 7. Same as Fig. 2 for the South Atlantic.

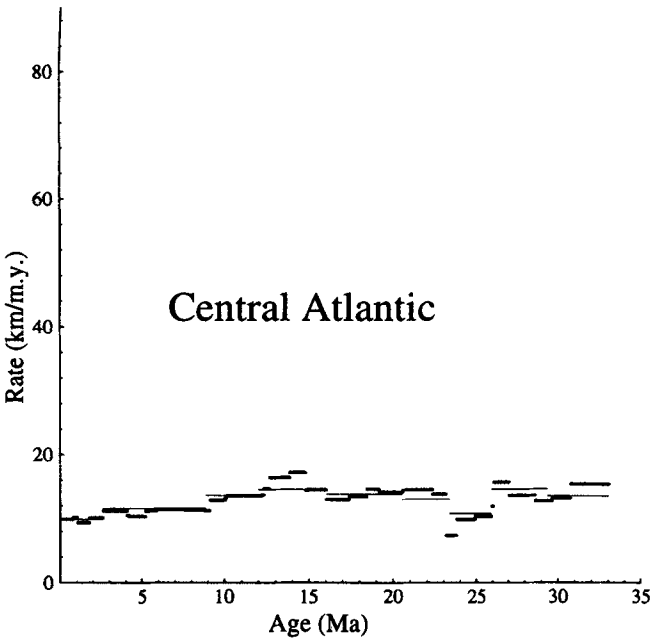

Figure 8. Same as Fig. 2 for the Central Atlantic.

Table 2. Residual sizes for ridge-crest rate functions ($km^2\ Ma^{-1}$).

	Cande & Kent	This study
EPR	474.8	443.1
Chile	933.1	807.7
S. Pac	314.2	275.4
N. Pac	4228.6	3072.9
SEIR	375.9	362.2
S. Atl	301.3	509.2
C. Atl	72.2	151.6
total	6700.1	5622.1

REFERENCES

Acton, G.D. & Huestis, S.P., 1994. Genetic algorithm optimizations for seafloor spreading rates and geomagnetic polarity time scales, *EOS, Trans., Am. Geophys. Un.*, **75**, 203.

Backus, G.E., 1988. Comparing hard and soft prior bounds in geophysical inverse problems, *Geophys. J. Int.*, **94**, 249–261.

Cande, S.C. & Kent, D.V., 1992. A new geomagnetic polarity time scale for the late Cretaceous and Cenozoic, *J. geophys. Res.*, **97**, 13 917–13 951.

Cande, S.C. & Kent, D.V., 1995. Revised calibration of the geomagnetic polarity timescale for the late Cretaceous and Cenozoic, *J. geophys. Res.*, **100**, 6093–6095.

Heirtzler, J.R., Dickson, G.O., Herron, E.M., Pitman, W.C. & LePichon, X, 1968. Marine magnetic anomalies, geomagnetic field reversals, and motions of the ocean floor and continents, *J. geophys. Res.*, **73**, 2119–2136.

Parker, R.L., 1994. *Geophysical Inverse Theory*, Princeton University Press, Princeton, NJ.

Press, W.H., Teukolsky, S.A., Vetterling, W.T. & Flannery, B.P., 1992. *Numerical Recipes in FORTRAN: the Art of Scientific Computing*, 2nd edn, Cambridge University Press, Cambridge.

Wilson, D.S., 1993. Confirmation of the astronomical calibration of the magnetic polarity timescale from sea-floor spreading rates, *Nature*, **364**, 788–790.